



Antibacterial prenylated stilbenoids from peanut (*Arachis hypogaea*)

de Bruijn, W. J. C., Araya-Cloutier, C., Bijlsma, J., de Swart, A., Sanders, M. G., de Waard, P., ... Vincken, J. P.

This is a "Post-Print" accepted manuscript, which has been published in  
"Phytochemistry Letters"

This version is distributed under a non-commercial no derivatives Creative Commons



([CC-BY-NC-ND](https://creativecommons.org/licenses/by-nc-nd/4.0/)) user license, which permits use, distribution, and reproduction in any medium, provided the original work is properly cited and not used for commercial purposes. Further, the restriction applies that if you remix, transform, or build upon the material, you may not distribute the modified material.

Please cite this publication as follows:

de Bruijn, W. J. C., Araya-Cloutier, C., Bijlsma, J., de Swart, A., Sanders, M. G., de Waard, P., ... Vincken, J. P. (2018). Antibacterial prenylated stilbenoids from peanut (*Arachis hypogaea*). *Phytochemistry Letters*, 28, 13-18. DOI: 10.1016/j.phytol.2018.09.004

You can download the published version at:

<https://doi.org/10.1016/j.phytol.2018.09.004>

# Antibacterial prenylated stilbenoids from peanut (*Arachis hypogaea*)

Wouter J. C. de Bruijn<sup>a</sup>, Carla Araya-Cloutier<sup>a</sup>, Judith Bijlsma<sup>a</sup>, Anne de Swart<sup>a</sup>, Mark G. Sanders<sup>a</sup>, Pieter de Waard<sup>b</sup>, Harry Gruppen<sup>a</sup>, Jean-Paul Vincken<sup>a\*</sup>

<sup>a</sup> Laboratory of Food Chemistry, Wageningen University, P.O. Box 17, 6700 AA Wageningen, The Netherlands

<sup>b</sup> MAGNEFY (MAGNEtic resonance research FacilitY), Wageningen University, Wageningen, The Netherlands

\* Corresponding author: e-mail [jean-paul.vincken@wur.nl](mailto:jean-paul.vincken@wur.nl); tel. +31 (0)317 482234

## 1 **Abstract**

2 Stilbenoids are a class of secondary metabolites with a stilbene backbone that can be produced  
3 by peanut (*Arachis hypogaea*) as defence metabolites. Six monomeric prenylated stilbenoids,  
4 including the compound arachidin-6 (**4**), were isolated from extracts of fungus-elicited peanuts  
5 (*Arachis hypogaea*) using preparative liquid chromatography. Their structures were confirmed  
6 by MS<sup>n</sup>, HRMS and NMR spectroscopy and their antibacterial activity was evaluated against  
7 methicillin-resistant *Staphylococcus aureus* (MRSA). Similarly to other phenolic compounds,  
8 prenylated derivatives of stilbenoids were more active than their non-prenylated precursors  
9 piceatannol, resveratrol, and pinosylvin. Chiricanine A (**6**), a chain-prenylated pinosylvin  
10 derivative, was the most potent compound tested, with a minimum inhibitory concentration  
11 (MIC) of 12.5 µg mL<sup>-1</sup>. Arachidin-6 (**4**), a ring-prenylated piceatannol derivative, had moderate  
12 potency (MIC 50-75 µg mL<sup>-1</sup>). In conclusion, prenylated stilbenoids represent a group of  
13 potential natural antibacterials which show promising activity against MRSA.

## 14 **Highlights**

- 15 • New stilbenoid: arachidin-6, a ring-prenylated piceatannol derivative.
- 16 • Antibacterial activity of purified prenylated stilbenoids assessed against MRSA.
- 17 • Chiricanine A (MIC 12.5 µg mL<sup>-1</sup>) and other stilbenoids are active against MRSA.

## 18 **Keywords**

19 Leguminosae, natural product, secondary metabolite, stilbene, prenylation, antimicrobial

## 20 **1. Introduction**

21 Stilbenoids, a class of secondary metabolites with a stilbene backbone (**Figure 1A**), can be  
22 produced by peanut (*Arachis hypogaea*) as defence metabolites (Sobolev, 2013). Analogous to  
23 phenolic metabolites of other members of the *Leguminosae* family, e.g. soy bean and mung  
24 bean (Aisyah et al., 2016; Simons et al., 2011), the production of stilbenoids and, in particular,  
25 their prenylated derivatives can be stimulated by fungal elicitation of germinating peanut seeds  
26 (Aisyah et al., 2015; Sobolev et al., 2016; Sobolev et al., 2010). Prenylation refers to the  
27 attachment of a prenyl-moiety (i.e. 3,3-dimethylallyl) by a prenyltransferase and in the case of  
28 peanut stilbenoids occurs mainly at the 4-position (Yang et al., 2016) as in, for example,  
29 arachidin-2 (**Figure 1B, compound 2**) (Sobolev et al., 2016). Prenylation of phenolic  
30 compounds has been shown to increase their antibacterial activity, which is exemplified by the  
31 minimum inhibitory concentrations (MICs) of genistein (MIC >128  $\mu\text{g mL}^{-1}$ ), 6-prenyl-  
32 genistein (MIC 32  $\mu\text{g mL}^{-1}$ ), and 6,8-diprenyl-genistein (MIC 8  $\mu\text{g mL}^{-1}$ ) against methicillin-  
33 resistant *Staphylococcus aureus* (MRSA) (Hatano et al., 2000). More generally, prenylated  
34 (iso)flavonoids have been shown to possess antibacterial activity against antibiotic-resistant  
35 strains of *S. aureus* and other pathogenic gram-positive bacteria (Araya-Cloutier et al., 2017;  
36 Araya-Cloutier et al., 2018a; Gibbons, 2004). An extract from fungus (*Rhizopus*) elicited peanut  
37 seedlings, enriched in prenylated stilbenoids, already showed promising antibacterial activity  
38 against *E. coli*, *L. monocytogenes* and MRSA (Araya-Cloutier et al., 2017; Araya-Cloutier et  
39 al., 2018b). In this study, we have isolated and characterized several prenylated compounds  
40 with different stilbenoid precursors and prenyl configurations from an extract of *Rhizopus*-  
41 elicited peanut seedlings and assessed their antibacterial activity against MRSA. In analogy  
42 with other phenolic compounds, we hypothesize that prenylation of stilbenoids will enhance  
43 their antibacterial activity.

## 44 **2. Results and discussion**

### 45 **2.1 Sample Clean-up, Pre-purification and Purification by Preparative RP-HPLC**

46 The crude extract of *Rhizopus*-elicited peanut seedlings showed a chromatographic profile on  
47 RP-UHPLC comparable to what was described previously (Aisyah et al., 2015). The clean-up  
48 with ethyl acetate effectively removed the majority of polar impurities in the extract, yielding  
49 the cleaned extract which contained mainly prenylated stilbenoids (**Figure S1**, supplementary  
50 data, 6-19 min) and apolar impurities (**Figure S1**, 19-28 min) which, based on LC-MS analysis,  
51 were mostly lipids like oxylipins and free fatty acids (Murphy, 2014). After pre-purification by  
52 Flash chromatography, most of the apolar impurities were removed and several pools were  
53 obtained enriched in mixtures of prenylated stilbenoids and some oxylipins (**Figure S1**). After  
54 subjecting these pools to preparative RP-HPLC separation, six purified compounds were  
55 obtained.

### 56 **2.2 Structure Elucidation of the Prenylated Stilbenoids**

57 The six compounds that were isolated were first analysed by UHPLC-PDA-ESI-IT-MS, the  
58 corresponding spectrometric and spectroscopic data of which is shown in **Table 1**. Based on  
59 the comparison of this data to literature (Aisyah et al., 2015; Sobolev et al., 2009; Sobolev et  
60 al., 2006), the compounds were tentatively annotated. For most purified compounds, the *trans*  
61 isomer was most abundant but the *cis* isomer was also present. The two isomers were  
62 distinguished by their  $\lambda_{\max}$ , and the peak with the higher  $\lambda_{\max}$  was assigned as the *trans* isomer,  
63 in accordance with previously reported data (Trela and Waterhouse, 1996). Based on UV<sub>310</sub>  
64 area compound **1** was approximately 60% *trans*, compound **3** was approximately 88% *trans*,  
65 and compounds **2**, **4**, **5** and **6** were all more than 97% *trans*. Spectrometric and spectroscopic  
66 data provided is based on the *trans* isomer.

67 In ESI-IT-MS (**Table 1**), the most abundant fragments observed for compounds **1-3** and **6** in  
68 negative ionisation mode were those with a neutral loss (NL) of 56 u (C<sub>4</sub>H<sub>8</sub>) and NL of 69 or

69 70 u, corresponding to complete loss of the prenyl chain (as C<sub>5</sub>H<sub>8</sub> or C<sub>5</sub>H<sub>9</sub>). In positive  
70 ionisation mode the main fragments were also related to the prenyl-moiety, resulting in a NL  
71 of 56 u (C<sub>4</sub>H<sub>8</sub>), as described previously for chain-prenylated (iso)flavonoids (Simons et al.,  
72 2009). For compounds **4** and **5** the main fragment observed in positive ionisation mode, *m/z*  
73 201, corresponded to loss of the catechol (NL 110 u, C<sub>6</sub>H<sub>4</sub>O<sub>2</sub>) or phenol (NL 94 u, C<sub>6</sub>H<sub>4</sub>O)  
74 moiety, respectively. Fragments corresponding to neutral losses of 56 u and 42 u were also  
75 observed. For compound **4** the fragment at *m/z* 269 (NL 42 u, rel. abundance 25) was more  
76 intense than the fragment at *m/z* 255 (NL 56 u, rel. abundance 13, not shown in **Table 1**). The  
77 same was observed for compound **5** with the fragments at *m/z* 253 (NL 42 u, rel. abundance 51)  
78 and *m/z* 239 (NL 56 u, rel. abundance 23). The abundance ratio of NL 42:56 u was > 1 for both  
79 compounds, indicating the presence of a ring prenyl rather than a chain prenyl (Simons et al.,  
80 2011). In negative ionisation mode, the prenyl-moiety of compounds **4** and **5** did not readily  
81 fragment, instead the unfragmented parent ion, radical fragments and small neutral losses like  
82 •CH<sub>3</sub> (15 u), H<sub>2</sub>O (18 u), CO (28 u), and CO<sub>2</sub> (44 u) were observed.

83 High resolution mass spectrometric data, as determined by UHPLC-ESI-FTMS, confirmed the  
84 expected molecular formulae of all six compounds (**Table 1**). To confirm the tentative  
85 annotations of the structures, <sup>1</sup>H NMR spectra of compounds **1-6** were acquired. The structure  
86 of compounds **1-3**, **5** and **6** was confirmed by comparison of their <sup>1</sup>H NMR spectra to published  
87 data (Chang et al., 2006; Park et al., 2011; Royer et al., 2010; Sobolev et al., 2009). Compound  
88 **4** (C<sub>19</sub>H<sub>18</sub>O<sub>4</sub> based on FTMS), however, which was previously tentatively annotated as 4-  
89 isopentadienyl-3,5,3',4'-tetrahydroxystilbene (IPP) based on UHPLC-PDA-ESI-IT-MS  
90 (Aisyah et al., 2015), did not match this compound's expected <sup>1</sup>H NMR spectrum. HMBC and  
91 HMQC were performed in order to elucidate the structure of compound **4** (see **Table 2** for the  
92 <sup>1</sup>H and <sup>13</sup>C NMR spectroscopic data). The <sup>13</sup>C NMR spectrum showed signals identical to those  
93 described for the catechol moiety of arachidin-1 (Chang et al., 2006). These signals were

94 thereby assigned as aromatic carbons C-1' to C-6'. Based on the HMBC and HMQC cross peaks  
95 of these carbons, the three  $^1\text{H}$  NMR signals at  $\delta_{\text{H}}$  6.974 (d,  $J = 2.0$  Hz, H-2'), 6.737 (d,  $J = 8.2$   
96 Hz, H-5'), and 6.835 (dd,  $J = 8.2$  and  $2.0$  Hz, H-6') were assigned as the corresponding protons.  
97 The olefin carbons C- $\alpha$  ( $\delta_{\text{C}}$  126.75) and C- $\alpha'$  ( $\delta_{\text{C}}$  129.69) showed HMQC cross peaks with two  
98 doublet proton signals at  $\delta_{\text{H}}$  6.721 ( $J = 16.2$  Hz, H- $\alpha$ ) and 6.889 ( $J = 16.2$  Hz, H- $\alpha'$ ), whose  
99 coupling constants confirmed the *trans*-olefin. Both of these protons showed cross peaks with  
100 aromatic carbons C-1' and C-1 ( $\delta_{\text{C}}$  140.23). Proton H- $\alpha$  also showed HMBC cross peaks with  
101  $^{13}\text{C}$  NMR signals  $\delta_{\text{C}}$  106.47 (C-6) and 106.79 (C-2). The  $^1\text{H}$  NMR signals  $\delta_{\text{H}}$  6.418 (bs, H-2)  
102 and 6.475 (d,  $J = 1.3$  Hz, H-6) were assigned by their HMQC cross peaks to C-2 and C-6,  
103 respectively. These chemical shifts and their HMBC cross peaks were comparable to those  
104 described for arahypin-5 (Sobolev et al., 2009). Analogous to arahypin-5 and arachidin-1 the  
105 carbon signal  $\delta_{\text{C}}$  110.23 (C-4) showed HMBC cross peaks with H-2 and H-6 and did not have  
106 any HMQC cross peaks, indicating that the prenyl was attached at C-4. The remaining  $^{13}\text{C}$  NMR  
107 signals were consistent with spectroscopic data of C-3 ( $\delta_{\text{C}}$  155.26), C-5 ( $\delta_{\text{C}}$  154.42) and the five  
108 carbons of the prenyl group reported for arahypin-5 (Sobolev et al., 2009). The signal of C-3''  
109 ( $\delta_{\text{C}}$  76.77) was downfield compared to arachidin-1, which indicated that the prenyl was cyclised  
110 to a pyran as in arahypin-5. The remaining  $^1\text{H}$  NMR signals and their HMBC cross peaks  
111 corresponded to those described for arahypin-5 (Sobolev et al., 2009). To the best of our  
112 knowledge the elucidated structure, a ring-prenylated piceatannol derivative, has not been  
113 previously reported. Consequently, compound **4** was identified as the new compound, 7-[(*E*)-  
114 2-(3,4-dihydroxyphenyl)ethenyl]-2,2-dimethylchromen-5-ol, herein named arachidin-6. The  
115 structures of compounds **1-6** are shown in **Figure 1B**.

116 Prenyl chains in (iso)flavonoids and chalcones have been described to be liable to cyclisation  
117 under acidic conditions (Popłoński et al., 2018; Singhal et al., 1980). Thus, it might be argued  
118 compound **4** might be an artefact formed due to the addition of 1% (*v/v*) formic acid in the

119 preparative chromatography eluent. Acid-catalysed cyclisation of a prenyl chain, however,  
120 typically yields a dihydropyran (Popłoński et al., 2018; Singhal et al., 1980), whereas the prenyl  
121 in compound **4** is present as a pyran as evidenced by the structure elucidation. It was, therefore,  
122 concluded that the compound as such was present in the elicited peanut seedlings.

### 123 **2.3 Stability and Antibacterial Activity of Prenylated Stilbenoids**

124 During the purification process, the prenylated stilbenoids were prone to both *trans-cis*  
125 isomerisation, as was previously reported (Trela and Waterhouse, 1996), and dimerization. The  
126 compounds' reactivity could potentially be of influence on their antimicrobial activity.  
127 Therefore, the stability of the compounds during the antibacterial assay was assessed by  
128 incubating them under normal assay conditions. Under these conditions, no further *trans* to *cis*  
129 isomerisation or dimerization was observed for compounds **2-6** (**Figure S2**, supplementary  
130 data). Arachidin-1 (**1**) was not included due to low amounts of available material. However, we  
131 assumed its stability during the assay would be similar to that of the other five compounds.  
132 Thus, we did not expect any influence of isomerization or dimerization on the antibacterial  
133 assay results.

134 The antibacterial activity of arachidin-1 (**1**), arachidin-2 (**2**), arachidin-3 (**3**), arachidin-6 (**4**),  
135 arahypin-5 (**5**), and chiricanine A (**6**) against MRSA was assessed. For reference, non-  
136 prenylated stilbenoids piceatannol (precursor of arachidin-1 (**1**) and -6 (**4**)), resveratrol  
137 (precursor of arachidin-2 (**2**) and -3 (**3**) and arahypin-5 (**5**)), and pinosylvin (precursor of  
138 chiricanine A (**6**)) were also tested. The resulting MIC and TTD values are shown in **Table 3**,  
139 together with some structural properties of these molecules. For resveratrol and piceatannol, no  
140 MIC was found below 200  $\mu\text{g mL}^{-1}$ . Therefore, they were considered not to be active  
141 antibacterials. The attachment of a prenyl-moiety to these precursors increased the resulting  
142 molecule's antibacterial activity, as expected. For example, resveratrol had an MIC of  $> 200$   
143  $\mu\text{g mL}^{-1}$  ( $> 877 \mu\text{M}$ ) and its ring-prenylated derivative arahypin-5 (**5**) had an MIC of 25-50  $\mu\text{g}$



144 mL<sup>-1</sup> (85-170 μM), thus the prenyl group enhanced activity by up to ten fold in this case. No  
145 MIC was found below 50 μg mL<sup>-1</sup> for arachidin-1 (**1**), arachidin-2 (**2**), or arachidin-3 (**3**). Based  
146 on the TTD<sub>50</sub> (time-to-detection at 50 μg mL<sup>-1</sup>) values of these compounds, arachidin-2 (**2**) was  
147 the most active of the three. In addition, the TTD<sub>50</sub> and TTD<sub>25</sub> values obtained for these  
148 compounds indicated that they were less active than compounds **4-6** and, especially arachidin-  
149 1 (**1**) and arachidin-3 (**3**), were only marginally more active than non-prenylated resveratrol and  
150 piceatannol. The new compound, arachidin-6 (**4**), showed moderate activity with MIC at 50-75  
151 μg mL<sup>-1</sup>. The prenylated pinosylvin derivative, chiricanine A (**6**), was the most active  
152 compound tested in this work with an observed MIC of 12.5 μg mL<sup>-1</sup> (44 μM) against MRSA,  
153 which is quite promising and in range of that of some traditional antibiotics (Braga et al., 2005).

#### 154 **2.4 Structure-Activity Relationships of Prenylated Stilbenoids against MRSA**

155 The antimicrobial activity of prenylated phenolics has been related to the increased  
156 hydrophobicity conferred by the addition of the prenyl-group (Botta et al., 2005). Chiricanine  
157 A (**6**) possessed the highest LogD<sub>7.2</sub> of the six purified compounds. The anti-MRSA activity of  
158 compounds **1-6** (expressed as TTD<sub>25</sub>, using 24 h if TTD > 24 h) was, however, not correlated  
159 to their LogD<sub>7.2</sub> (r = 0.002). The lack of a correlation between activity and hydrophobicity has  
160 been previously described for prenylated phenolic compounds (Araya-Cloutier et al., 2018b).  
161 The configuration of the prenyl-moiety (chain or ring) seems to have an effect on the observed  
162 antibacterial activity. Ring prenylation was found to be more effective than chain prenylation,  
163 as demonstrated when comparing molecules with the same stilbenoid precursor: arachidin-1 (**1**)  
164 (chain, TTD<sub>25</sub> 6.1 h) vs. arachidin-6 (**4**) (ring, TTD<sub>25</sub> 11.5 h) and arachidin-2 (**2**) or -3 (**3**) (chain,  
165 TTD<sub>25</sub> 7.4 or 6.6 h, respectively) vs. arahypin-5 (**5**) (ring, TTD<sub>25</sub> 9.6 – >24 h) (**Table 3**). This  
166 was in contrast with previous results which indicated that chain-prenylated (iso)flavonoids were  
167 generally more active than ring-prenylated ones (Araya-Cloutier et al., 2018a; Araya-Cloutier  
168 et al., 2018b). The effect of a 3-methyl-1-butene (arachidin-1 (**1**) and -3 (**3**)) or a 3-methyl-2-

169 butene (arachidin-2 (**2**)) type prenyl chain was not completely clear but the higher TTD<sub>50</sub> of  
170 arachidin-2 indicated that a 3-methyl-2-butene chain might result in better activity than a 3-  
171 methyl-1-butene chain.

172 The stilbenoid precursor of the prenylated compounds might also affect their activity. So far,  
173 our results indicated that the order of activity for the three tested precursors is pinosylvin >  
174 resveratrol > piceatannol. Within the group of compounds **1-6**, the number of hydrogen bond  
175 donors is negatively correlated with TTD<sub>25</sub> ( $r = -0.89$ ), i.e. having less hydrogen bond donors  
176 seems to result in better anti-MRSA activity. This matches previously described results for  
177 pterostilbene (i.e. 3,5-dimethyl-resveratrol, MIC 78  $\mu$ M) which was found to be up to 16 times  
178 more active against MRSA than resveratrol in that study (MIC 1,250  $\mu$ M) (Yang et al., 2017).

179 The structure-antibacterial activity relationships described above indicate that prenylated  
180 stilbenoids from the pinosylvin precursor seem to be most potent. In addition, ring prenylation  
181 seems to confer more antibacterial potential than chain prenylation. A candidate anti-MRSA  
182 molecule reported in literature would be arahypin-13 (ring-prenylated pinosylvin) (Sobolev et  
183 al., 2016). This molecule might show similar or even more potent activity than chiricanine A.  
184 To establish quantitative structure-activity relationships, evaluation of a larger set of  
185 compounds will be necessary.

### 186 **3. Conclusion**

187 Similarly to other phenolic compounds, prenylation of stilbenoids enhances their antibacterial  
188 activity. Prenylated stilbenoids represent a group of natural potential antibacterials with activity  
189 against the antibiotic-resistant gram-positive bacterium MRSA. The newly discovered  
190 prenylated stilbenoid, arachidin-6, was moderately potent with an MIC of 50-75  $\mu\text{g mL}^{-1}$   
191 against MRSA, whereas the activity of chiricanine A, with its MIC of 12.5  $\mu\text{g mL}^{-1}$ , is in range  
192 with some traditional antibiotics. Within the set of stilbenoids assessed in this work prenylation  
193 enhanced antimicrobial activity. Hydrophobicity was not correlated with antimicrobial activity,  
194 whereas ring-prenylation seems to convey a larger increase in activity than chain-prenylation.

## 195 **4. Experimental**

### 196 **4.1 General Experimental Procedures**

197 NMR Spectra were recorded on a Bruker Avance-III-600 spectrometer, equipped with a cryo-  
198 probe. Compounds **1**, **2**, **4**, and **5** were dissolved in 0.5 mL methanol-d<sub>4</sub> (99.9 atom%, Isotec);  
199 compounds **3** and **6** were dissolved in 0.5 mL chloroform-d (99.9 atom%, Isotec). <sup>1</sup>H and <sup>13</sup>C  
200 NMR spectra were recorded at a probe temperature of 300 K. Chemical shifts are expressed in  
201 ppm relative to internal TMS at 0.00 ppm, but were actually measured to the residual solvent  
202 signals of methanol ( $\delta\text{C} = 49.00$  ppm,  $\delta\text{H} = 3.31$  ppm) or chloroform ( $\delta\text{C} = 77.16$  ppm,  $\delta\text{H} =$   
203  $7.26$  ppm). For all compounds, 1D <sup>1</sup>H spectra were acquired. For compound **4**, additional 1D  
204 <sup>13</sup>C and 2D COSY, HMBC, and HMQC spectra were acquired. ESI-IT-MS<sup>n</sup> spectra were  
205 acquired on an LTQ Velos Pro linear ion trap mass spectrometer (Thermo Scientific, San Jose,  
206 CA, USA) equipped with a heated ESI probe coupled *in-line* to the Accela RP-UHPLC system  
207 (Thermo Scientific). The Accela UHPLC system was used in the same configuration as  
208 previously described (de Bruijn et al., 2016). The flow rate was 300  $\mu\text{L min}^{-1}$  at a column  
209 temperature of 35 °C. Eluents used were water (A) and MeOH (B), both with 0.1% (v/v) formic  
210 acid. The elution profile can be found in the supplementary data. Detection wavelengths for  
211 UV-Vis were set to the range of 200-600 nm and data were recorded at 20 Hz. High resolution  
212 mass data were acquired on a Thermo Q Exactive Focus hybrid quadrupole-orbitrap mass  
213 spectrometer (Thermo Scientific) equipped with a heated ESI probe (ESI-FTMS) coupled *in-*  
214 *line* to the Vanquish RP-UHPLC system. The Vanquish UHPLC system (Thermo Scientific) in  
215 the same configuration and with the same column as described previously (de Bruijn et al.,  
216 2016). The samples were eluted with water (A) and ACN (B), both with 0.1% (v/v) formic acid  
217 with a flow rate of 400  $\mu\text{L min}^{-1}$  at 45 °C. The elution profile can be found in the supplementary  
218 data. A Waters Acquity BEH C18 2.1  $\times$  150 mm, 1.7  $\mu\text{m}$  particle size column with a Waters  
219 VanGuard 2.1  $\times$  5 mm guard column of the same material was used for all analytical RP-

220 UHPLC separations. Flash chromatography was performed on a Reveleris Flash  
221 chromatography system (Grace, Columbia, MD, USA). A Reveleris C18 RP 80 g cartridge  
222 (particle size 40  $\mu\text{m}$ ) was eluted with water (A) and MeOH (B), both with 1% (v/v) formic acid,  
223 at room temperature at a flow rate of 60 mL min<sup>-1</sup>. Preparative chromatography was performed  
224 on a Waters preparative RP-HPLC-MS system (Waters, Milford, MA, USA) as previously  
225 described (van de Schans et al., 2016). The column used was a Waters XBridge Prep C18 OBD  
226 column (19  $\times$  250 mm, 5  $\mu\text{m}$  particle size) and was eluted with water (A) and ACN (B), both  
227 with 1% (v/v) formic acid, at room temperature at a flow rate of 17 mL min<sup>-1</sup>.

## 228 **4.2 Chemicals**

229 Sodium hypochlorite 47/50% (w/v) solution (~13% active Cl) was obtained from Chem-Lab  
230 (Zedelgem, Belgium). Technical grade *n*-hexane 98% (v/v) was obtained from VWR  
231 International (Radnor, PA, USA). UHPLC-MS grade solvents and HPLC grade ACN (for  
232 preparative chromatography) were purchased from Biosolve (Valkenswaard, The Netherlands).  
233 *trans*-Piceatannol >98% (w/w) and *trans*-resveratrol  $\geq$ 98% (w/w) were purchased from Cayman  
234 Chemical (Ann Arbor, MI, USA). *trans*-Pinosylvin  $\geq$ 97% (w/w) and *tert*-butanol  $\geq$ 98% (w/w)  
235 were purchased from Sigma-Aldrich (St. Louis, MO, USA). Water (MQ) for other purposes  
236 than UHPLC was prepared using a Milli-Q water purification system (Merck Millipore,  
237 Billerica, MA, USA). Ethanol absolute  $\geq$ 99.9% (v/v) was purchased from Merck Millipore.

## 238 **4.3 Plant and Fungal Material**

239 Peeled peanuts (*Arachis hypogaea*) with skin for feed purposes were purchased locally. Dried  
240 *Rhizopus* culture was purchased as tempeh starter culture from TopCultures (Zoersel, Belgium).

#### 241 **4.4 Peanut Germination and Elicitation with *Rhizopus***

242 Peanuts were surface-sterilized by soaking in a 1% (w/v) hypochlorite solution (5 L kg<sup>-1</sup> seeds)  
243 for 15 min at room temperature and were then rinsed with demineralized water. Surface-  
244 sterilized peanuts were germinated in the dark in a pilot-scale two-tank steep germinator  
245 (Custom Laboratory Products, Keith, UK). The cleaning procedure, trays, and setup of the  
246 germinator were the same as described previously (de Bruijn et al., 2016). In total 3 kg of  
247 peanuts were germinated in two identical experiments. Approximately 300 g peanuts were  
248 placed in each of the five tray compartments that were lined with disinfected cellulose filter  
249 paper (Whatman 595 ½, folded, 320 mm). The program set in the germinator was as follows:  
250 soaking for 16 h at 25 °C (aeration 1 min every 10 min), followed by germination for 48 h at 25  
251 °C. The germinating peanuts were then inoculated by pouring the *Rhizopus* starter culture (0.2  
252 L kg<sup>-1</sup> peanuts equalling approximately  $2 \times 10^5$  CFU g<sup>-1</sup> peanuts) over them. Prior to  
253 application, the starter culture was rehydrated with peptone physiological salt solution (Tritium  
254 Microbiologie, Eindhoven, The Netherlands) (100 mg mL<sup>-1</sup>) and incubated for 1 h at 37 °C.  
255 After fungal inoculation, peanuts were incubated for 72 h at 30 °C. During the entire process,  
256 relative humidity (RH) was controlled by periodical aeration with humidified air, RH of the air  
257 supplied to the tanks was maintained between 60-83% (monitored by germinator), resulting in  
258 RH of 82-95% inside the tanks (measured externally). The described conditions proved to be  
259 effective to ensure germination of the seeds as well as growth of the fungus. At the end of the  
260 experiment, the peanuts were frozen and stored at -20 °C until further processing.

#### 261 **4.5 Extraction and Isolation**

262 Peanut seedlings were extracted according to a method adapted from Sobolev and co-  
263 workers.(Sobolev et al., 2009) In short, the elicited peanut seedlings were defatted by  
264 continuous Soxhlet extraction with *n*-hexane for 5 h. The defatted peanut seedlings were then  
265 extracted with MeOH in a blender for 1 min (1 L MeOH per 200 g seedlings). The suspension

266 was filtered over a paper filter under reduced pressure and the retentate peanut pulp was  
267 subjected to one more identical extraction. The methanolic extracts were combined and defatted  
268 once more by liquid-liquid partitioning with *n*-hexane (hexane:MeOH, 1:3). The defatted  
269 methanolic extract was filtered over cellulose filter paper (Whatman 595 ½, folded, 320 mm)  
270 and the MeOH was evaporated under reduced pressure to yield the crude extract. Exposure to  
271 light was avoided where possible during further sample preparation and purification. In order  
272 to remove polar impurities, the dried crude extract was then suspended in ethyl acetate (33 mg  
273 mL<sup>-1</sup>), subjected to an ultrasonic bath for 10 min, and centrifuged (10 min, 4,000 × *g*). The  
274 supernatant, containing the prenylated stilbenoids, was collected while the pellet, containing  
275 mostly polar impurities, was discarded. The supernatant was evaporated to dryness under  
276 reduced pressure, recollected using *tert*-butanol and lyophilised to yield the cleaned extract.  
277 Cleaned extracts were pre-purified using Flash chromatography. The sample was solubilised in  
278 MeOH acidified with 1% (*v/v*) FA (final sample concentration 300-500 mg mL<sup>-1</sup>) and was  
279 manually injected (1.0-2.5 g per run). The elution profile used can be found in the  
280 supplementary data. The collected fractions were analysed by RP-UHPLC-PDA-ESI-IT-MS<sup>n</sup>  
281 and those containing similar compounds were pooled. The MeOH was removed under reduced  
282 pressure and the remaining water was removed by lyophilisation.

283 The pools obtained from Flash chromatography were further purified using a Waters  
284 preparative RP-HPLC system (Waters, Milford, MA, USA) as previously described (van de  
285 Schans et al., 2016). Pools were solubilised at 2 mg mL<sup>-1</sup> in 50% (*v/v*) aqueous MeOH and  
286 injected (2.0-2.5 mL) on a Waters XBridge Prep C18 OBD column (19 × 250 mm, 5 µm particle  
287 size) and were eluted with water (A) and ACN (B), both with 1% (*v/v*) formic acid, at room  
288 temperature at a flow rate of 17 mL min<sup>-1</sup>. The elution profile used for each compound can be  
289 found in the supplementary data. Data was acquired and analysed by MassLynx (version 4.1,  
290 Waters). The collected fractions were analysed by RP-UHPLC-PDA-ESI-IT-MS<sup>n</sup>. Based on

291 the analysis, fractions containing the same compound were pooled and the ACN was evaporated  
292 under a stream of N<sub>2</sub>. The remaining water phase was immediately frozen and lyophilised.

#### 293 **4.6 Micro-Broth Dilution Assay**

294 Compounds **1-6** were tested for their antibacterial activity against the gram-positive bacterium  
295 methicillin-resistant *Staphylococcus aureus* (MRSA) (18HN, spa type t034; RIVM, Bilthoven,  
296 The Netherlands), according to a previously described method (Araya-Cloutier et al., 2017).  
297 The final inoculum size used was  $4.2 \pm 0.2 \log_{10}$  CFU mL<sup>-1</sup>. Final concentrations tested ranged  
298 from 6.25 to 200 µg mL<sup>-1</sup>, depending on the amount of material available, with a maximum of  
299 2.1% (v/v) ethanol in the final solution. Stock solutions of the tested compounds were prepared  
300 in 70% (v/v) aqueous ethanol. Prior to the micro-broth dilution assay, the stocks were diluted  
301 in tryptone soy broth (TSB) (Oxoid, Basingstoke, UK). Equal volumes (100 µL) of the diluted  
302 compound and of inoculum were transferred to each well of a 96-well plate. Inoculum with  
303 vancomycin (VWR International) (final concentration of 4 µg mL<sup>-1</sup>) was used as a positive  
304 control. Inoculum with sterile TSB containing 2.1% (v/v) ethanol was used as a negative  
305 control. All compounds were tested in at least two independent biological replicates. The 96-  
306 well plate was covered with a gas-permeable imaging seal (4Tititude, Wotton, UK) and incubated  
307 in a SpectraMax M2e (Molecular Devices, Sunnyvale, CA, USA) at 37 °C for 24 h with  
308 constant linear shaking. The optical density at 600 nm (OD<sub>600</sub>) was measured every 5 min.  
309 Time-to-detection (TTD) was defined as the time (h) to reach a difference of 0.05 units from  
310 the initial OD<sub>600</sub> (Araya-Cloutier et al., 2017; Araya-Cloutier et al., 2018b). If no measurable  
311 increase in OD<sub>600</sub> was observed, the TTD was defined as >24 h and the tested concentration  
312 was considered to be inhibitory. The minimum inhibitory concentration (MIC) was defined as  
313 the lowest concentration of each compound that was found to be inhibitory. The TTD of the  
314 negative control with 2.1% (v/v) ethanol was 5.6 h (standard deviation  $\pm$  0.1 h) (average of four



315 independent biological replicates, each with triplicates). For comparison of the compounds,  
316 TTD at concentrations of 25 and 50  $\mu\text{g mL}^{-1}$ , respectively TTD<sub>25</sub> and TTD<sub>50</sub>, were determined.

317 **Supplementary data**

318 Elution profiles used for preparative and analytical liquid chromatography. UHPLC-ESI-IT-  
319 MS chromatograms of cleaned peanut extract and Flash pools (**Figure S1**). UHPLC-PDA  
320 chromatogram stability assessment of compounds **2-6** under antibacterial assay conditions  
321 (**Figure S2**).

## 322 References

- 323 Aisyah, S., Gruppen, H., Andini, S., Bettonvil, M., Severing, E., Vincken, J.-P., 2016. Variation in accumulation  
 324 of isoflavonoids in Phaseoleae seedlings elicited by *Rhizopus*. *Food Chem.* 196, 694-701.
- 325 Aisyah, S., Gruppen, H., Slager, M., Helmink, B., Vincken, J.-P., 2015. Modification of prenylated stilbenoids in  
 326 peanut (*Arachis hypogaea*) seedlings by the same fungi that elicited them: The fungus strikes back. *J. Agric. Food*  
 327 *Chem.* 63, 9260-9268.
- 328 Araya-Cloutier, C., den Besten, H. M. W., Aisyah, S., Gruppen, H., Vincken, J.-P., 2017. The position of  
 329 prenylation of isoflavonoids and stilbenoids from legumes (Fabaceae) modulates the antimicrobial activity against  
 330 Gram positive pathogens. *Food Chem.* 226, 193-201.
- 331 Araya-Cloutier, C., Vincken, J.-P., van de Schans, M. G. M., Hageman, J., Schaftenaar, G., den Besten, H. M. W.,  
 332 Gruppen, H., 2018a. QSAR-based molecular signatures of prenylated (iso)flavonoids underlying antimicrobial  
 333 potency against and membrane-disruption in Gram positive and Gram negative bacteria. *Sci. Rep.* 8, 9267.
- 334 Araya-Cloutier, C., Vincken, J.-P., van Ederen, R., den Besten, H. M. W., Gruppen, H., 2018b. Rapid membrane  
 335 permeabilization of *Listeria monocytogenes* and *Escherichia coli* induced by antibacterial prenylated phenolic  
 336 compounds from legumes. *Food Chem.* 240, 147-155.
- 337 Botta, B., Vitali, A., Menendez, P., Misiti, D., Delle Monache, G., 2005. Prenylated flavonoids: Pharmacology  
 338 and biotechnology. *Curr. Med. Chem.* 12, 713-739.
- 339 Braga, L. C., Leite, A. A. M., Xavier, K. G. S., Takahashi, J. A., Bemquerer, M. P., Chartone-Souza, E.,  
 340 Nascimento, A. M. A., 2005. Synergic interaction between pomegranate extract and antibiotics against  
 341 *Staphylococcus aureus*. *Can. J. Microbiol.* 51, 541-547.
- 342 Chang, J. C., Lai, Y. H., Djoko, B., Wu, P. L., Liu, C. D., Liu, Y. W., Chiou, R. Y. Y., 2006. Biosynthesis  
 343 enhancement and antioxidant and anti-inflammatory activities of peanut (*Arachis hypogaea* L.) arachidin-1,  
 344 arachidin-3, and isopentadienylresveratrol. *J. Agric. Food Chem.* 54, 10281-10287.
- 345 de Bruijn, W. J. C., Vincken, J.-P., Duran, K., Gruppen, H., 2016. Mass spectrometric characterization of  
 346 benzoxazinoid glycosides from *Rhizopus*-elicited wheat (*Triticum aestivum*) seedlings. *J. Agric. Food Chem.* 64,  
 347 6267-6276.
- 348 Gibbons, S., 2004. Anti-staphylococcal plant natural products. *Nat. Prod. Rep.* 21, 263-277.
- 349 Hatano, T., Shintani, Y., Aga, Y., Shiota, S., Tsuchiya, T., Yoshida, T., 2000. Phenolic constituents of licorice.  
 350 VIII. Structures of glicophenone and glicoisoflavanone, and effects of licorice phenolics on methicillin-resistant  
 351 *Staphylococcus aureus*. *Chem. & Pharm. Bull.* 48, 1286-1292.
- 352 Murphy, R. C., 2014. Chapter 1: Fatty acids. In: Murphy, R. C. (Ed.), *Tandem mass spectrometry of lipids:*  
 353 *Molecular analysis of complex lipids.* The Royal Society of Chemistry, Cambridge, UK, pp. 1-39.
- 354 Park, B. H., Lee, H. J., Lee, Y. R., 2011. Total synthesis of chiricanine A, arahypin-1, *trans*-arachidin-2, *trans*-  
 355 arachidin-3, and arahypin-5 from peanut seeds. *J. Nat. Prod.* 74, 644-649.
- 356 Popłoński, J., Turlej, E., Sordon, S., Tronina, T., Bartmańska, A., Wietrzyk, J., Huszcza, E., 2018. Synthesis and  
 357 antiproliferative activity of minor hops prenylflavonoids and new insights on prenyl group cyclization. *Molecules*  
 358 23.
- 359 Royer, M., Herbette, G., Eparvier, V., Beauchene, J., Thibaut, B., Stien, D., 2010. Secondary metabolites of  
 360 *Bagassa guianensis* Aubl. Wood: A study of the chemotaxonomy of the Moraceae family. *Phytochemistry* 71,  
 361 1708-1713.
- 362 Simons, R., Vincken, J.-P., Bakx, E. J., Verbruggen, M. A., Gruppen, H., 2009. A rapid screening method for  
 363 prenylated flavonoids with ultra-high-performance liquid chromatography/electrospray ionisation mass  
 364 spectrometry in licorice root extracts. *Rapid Commun. Mass Spectrom.* 23, 3083-3093.
- 365 Simons, R., Vincken, J.-P., Roidos, N., Bovee, T. F. H., van Iersel, M., Verbruggen, M. A., Gruppen, H., 2011.  
 366 Increasing soy isoflavonoid content and diversity by simultaneous malting and challenging by a fungus to  
 367 modulate estrogenicity. *J. Agric. Food Chem.* 59, 6748-6758.
- 368 Singhal, A. K., Sharma, R. P., Thyagarajan, G., Herz, W., Govindan, S. V., 1980. New prenylated isoflavones and  
 369 a prenylated dihydroflavonol from *Millettia pachycarpa*. *Phytochemistry* 19, 929-934.
- 370 Sobolev, V. S., 2013. Production of phytoalexins in peanut (*Arachis hypogaea*) seed elicited by selected  
 371 microorganisms. *J. Agric. Food Chem.* 61, 1850-1858.
- 372 Sobolev, V. S., Krausert, N. M., Gloer, J. B., 2016. New monomeric stilbenoids from peanut (*Arachis hypogaea*)  
 373 seeds challenged by an *Aspergillus flavus* strain. *J. Agric. Food Chem.* 64, 579-584.
- 374 Sobolev, V. S., Neff, S. A., Gloer, J. B., 2009. New stilbenoids from peanut (*Arachis hypogaea*) seeds challenged  
 375 by an *Aspergillus caelatus* strain. *J. Agric. Food Chem.* 57, 62-68.
- 376 Sobolev, V. S., Neff, S. A., Gloer, J. B., 2010. New dimeric stilbenoids from fungal-challenged peanut (*Arachis*  
 377 *hypogaea*) seeds. *J. Agric. Food Chem.* 58, 875-881.
- 378 Sobolev, V. S., Potter, T. L., Horn, B. W., 2006. Prenylated stilbenes from peanut root mucilage. *Phytochem. Anal.*  
 379 17, 312-322.

380 Trela, B. C., Waterhouse, A. L., 1996. Resveratrol: Isomeric molar absorptivities and stability. *J. Agric. Food*  
381 *Chem.* 44, 1253-1257.

382 van de Schans, M. G. M., Vincken, J.-P., de Waard, P., Hamers, A. R. M., Bovee, T. F. H., Gruppen, H., 2016.  
383 Glyceollins and dehydroglyceollins isolated from soybean act as SERMs and ER subtype-selective  
384 phytoestrogens. *J. Steroid Biochem. Mol. Biol.* 156, 53-63.

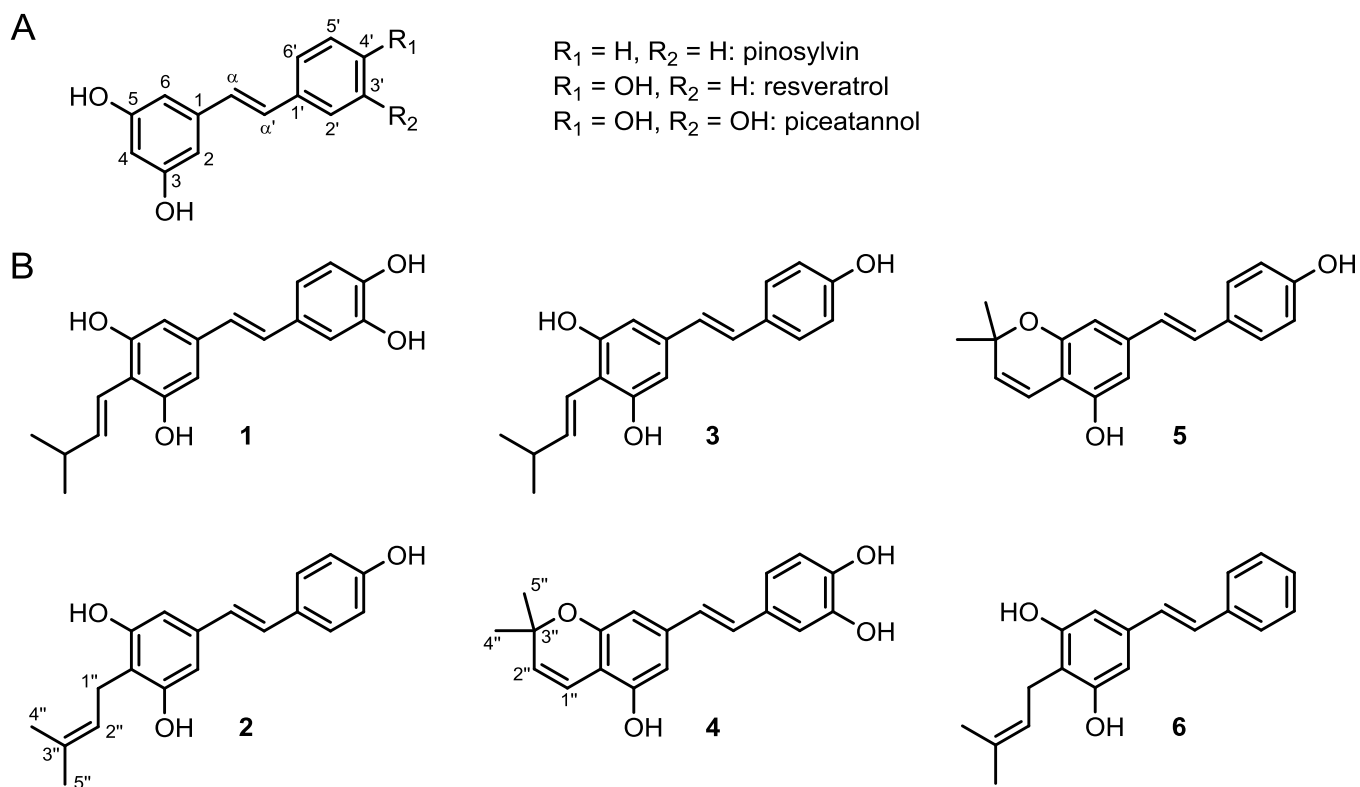
385 Yang, S. C., Tseng, C. H., Wang, P. W., Lu, P. L., Weng, Y. H., Yen, F. L., Fang, J. Y., 2017. Pterostilbene, a  
386 methoxylated resveratrol derivative, efficiently eradicates planktonic, biofilm, and intracellular MRSA by topical  
387 application. *Front. Microbiol.* 8, Article 1103.

388 Yang, T., Fang, L., Rimando, A. M., Sobolev, V., Mockaitis, K., Medina-Bolivar, F., 2016. A stilbenoid-specific  
389 prenyltransferase utilizes dimethylallyl pyrophosphate from the plastidic terpenoid pathway. *Plant Physiol.* 171,  
390 2483-2498.

391

392

393 **Figures**



394

395 **Figure 1.** A, natural stilbenoids with a stilbene backbone. B, prenylated stilbenoids isolated in  
 396 this work: **1**, arachidin-1; **2**, arachidin-2; **3**, arachidin-3; **4**, arachidin-6; **5**, arahypin-5; and **6**,  
 397 chiricanine A.

398 **Table 1.** Spectrometric and spectroscopic data of purified compounds as determined by UHPLC-PDA coupled to ESI-IT-MS and ESI-FTMS.

compound <sup>a</sup>	$\lambda_{\max}$ (nm)	ionisation	IT-MS			FTMS			
			$m/z$ precursor	MS <sup>2</sup> product ions (relative abundance) <sup>b</sup>	molecular formula	$m/z$ calc.	$m/z$ obs. <sup>c</sup>	error (ppm)	
<b>1</b>	339	[M-H] <sup>-</sup>	311	<u>241</u> , 242 (93), 312 (76), 255 (46), 267 (45), 311 (31), 293 (25), 224 (20), 172 (16)	C <sub>19</sub> H <sub>20</sub> O <sub>4</sub>	311.12888	311.12907	0.60	
		[M+H] <sup>+</sup>	313	<u>257</u>					
<b>2</b>	322	[M-H] <sup>-</sup>	295	239, 296 (55), 240 (43), 226 (42), 295 (38)	C <sub>19</sub> H <sub>20</sub> O <sub>3</sub>	295.13397	295.13388	-0.30	
		[M+H] <sup>+</sup>	297	<u>241</u>					
<b>3</b>	338	[M-H] <sup>-</sup>	295	<u>239</u> , 240 (48), 226 (31), 295 (26), 227 (25), 251 (18)	C <sub>19</sub> H <sub>20</sub> O <sub>3</sub>	295.13397	295.13402	0.18	
		[M+H] <sup>+</sup>	297	<u>241</u>					
<b>4</b>	342	[M-H] <sup>-</sup>	309	<u>309</u> , 310 (63), 265 (60), 291 (24), 294 (21), 281 (18)	C <sub>19</sub> H <sub>18</sub> O <sub>4</sub>	309.11323	309.11334	0.35	
		[M+H] <sup>+</sup>	311	<u>201</u> , 283 (55), 135 (50), 187 (40), 177 (30), 293 (29), 123 (28), 269 (25), 175 (22), 183 (20), 173 (19), 265 (17), 189 (16), 202 (16)					
<b>5</b>	339	[M-H] <sup>-</sup>	293	<u>293</u> , 278 (47), 294 (35)	C <sub>19</sub> H <sub>18</sub> O <sub>3</sub>	293.11832	293.11847	0.52	
		[M+H] <sup>+</sup>	295	<u>201</u> , 267 (93), 253 (51), 175 (37), 107 (37), 277 (32), 183 (28), 225 (24), 239 (23), 173 (19), 159 (18), 119 (18), 249 (15)					
<b>6</b>	312	[M-H] <sup>-</sup>	279	<u>224</u> , 223 (85), 279 (66), 280 (50), 211 (15)	C <sub>19</sub> H <sub>20</sub> O <sub>2</sub>	279.13905	279.13914	0.31	
		[M+H] <sup>+</sup>	281	<u>225</u>					

399 <sup>a</sup> Data provided based on the *trans* isomer.

400 <sup>b</sup> Most abundant fragment is underlined, only fragment ions with a relative abundance of at least 15 are shown.

401 <sup>c</sup> Based on the average of 5 spectra in negative ionisation mode.

402 **Table 2.**  $^1\text{H}$  (600 MHz) and  $^{13}\text{C}$  (150 MHz) NMR Spectroscopic data of arachidin-6 (**4**)  
 403 recorded in methanol- $\text{d}_4$  at 300K ( $\delta$  in ppm,  $J$  in Hz).

arachidin-6 ( <b>4</b> )		
position	$\delta_{\text{C}}$ , type	$\delta_{\text{H}}$ , mult. ( $J$ in Hz) <sup>a</sup>
1	140.23, C	
2	106.79, CH	6.418, bs
3	155.26, C	
4	110.23, C	
5	154.42, C	
6	106.47, CH	6.475, d (1.3)
$\alpha$	126.75, CH	6.721, d (16.2)
$\alpha'$	129.69, CH	6.889, d (16.2)
1'	131.02, C	
2'	113.83, CH	6.974, d (2.0)
3'	146.51, C	
4'	146.60, C	
5'	116.43, CH	6.737, d (8.2)
6'	120.27, CH	6.835, dd (8.2, 2.0)
1''	118.23, CH	6.626, d (9.9)
2''	129.10, CH	5.568, d (9.8)
3''	76.77, C	
4''	28.01, $\text{CH}_3$	1.391, s
5''	28.01, $\text{CH}_3$	1.391, s

404 <sup>a</sup> bs, broad singlet; d, doublet; dd, doublet of doublets; s, singlet.

**Table 3.** Structural characteristics, purity, and antibacterial activity of piceatannol, resveratrol, pinosylvin and the purified prenylated stilbenoids against MRSA.

compound	precursor	prenyl configuration, type	no. of H-bond donors	LogD <sub>7.2</sub> <sup>a</sup>	purity (%) <sup>b</sup>			MIC (µg mL <sup>-1</sup> )	TTD <sub>25</sub> (± StDev) (h) <sup>c</sup>	TTD <sub>50</sub> (± StDev) (h) <sup>c</sup>
					UV <sub>310</sub>	MS (NI)	<sup>1</sup> H NMR			
Piceatannol	n.a.	n.a.	n.a.	3.06	99	99	n.d.	>200	5.4 (± 0.1)	6.3 (± 0.3)
Resveratrol	n.a.	n.a.	n.a.	3.38	≥99	98	n.d.	>200	6.0 (± 0.1)	6.9 (± 0.7)
Pinosylvin	n.a.	n.a.	n.a.	3.69	≥99	≥99	n.d.	≤100 <sup>d</sup>	n.d. <sup>d</sup>	n.d. <sup>d</sup>
Arachidin-1	pice	chain, 3m1b	4	4.93	87	88	80	>50	6.1 (± 0.6)	8.4 (± 0.5)
Arachidin-2	resv	chain, 3m2b	3	5.10	98	89	95	>50	7.4 (± 0.5)	17.1 (± 3.0)
Arachidin-3	resv	chain, 3m1b	3	5.23	80	63	60	>50	6.6 (± 1.2)	8.6 (± 1.8)
Arachidin-6	pice	ring	3	4.27	96	96	n.d.	50-75 <sup>e</sup>	11.5 (± 2.2)	21.5 (± 0.5) – >24 <sup>e</sup>
Arahypin-5	resv	ring	2	4.58	99	94	80	25-50 <sup>e</sup>	9.6 (± 4.2) – >24 <sup>e</sup>	>24 (± n.a.)
Chiricanine A	pino	chain, 3m2b	2	5.40	99	98	99	12.5 <sup>e</sup>	>24 (± n.a.)	>24 (± n.a.)

n.a., not applicable; n.d., not determined; resv., resveratrol; pice, piceatannol; pino, pinosylvin; 3m1b, 3-methyl-1-butene, 3m2b; 3-methyl-2-butene.

<sup>a</sup> LogD<sub>7.2</sub>, calculated octanol-water partitioning coefficient at pH 7.2, as calculated using MarvinSketch 17.2.27 with default settings.

<sup>b</sup> Combined purity of the *trans* and *cis* isomers of the purified compounds. UV<sub>310</sub>, based on total peak area in UHPLC-PDA at 310 nm; MS (NI), based on total peak area in UHPLC-ESI-MS negative ionisation mode (*m/z* range 200-1500); <sup>1</sup>H NMR, based on the aromatic region in proton NMR spectroscopy.

<sup>c</sup> TTD<sub>25</sub>, time-to-detection at 25 µg mL<sup>-1</sup>; TTD<sub>50</sub>, time-to-detection at 50 µg mL<sup>-1</sup>.

<sup>d</sup> Pinosylvin was only tested in the concentration range 100-400 µg mL<sup>-1</sup> (one biological experiment, triplicate measurement).

<sup>e</sup> Determined in four independent biological replicates, ranges indicate that MIC and TTD varied between experiments.



## **Elution profiles reversed-phase chromatography**

### **Pre-purification by RP-Flash Chromatography**

For Flash chromatography, samples were injected on a Reveleris C18 RP 80 g cartridge (particle size 40  $\mu\text{m}$ ) and eluents used were water (A) and MeOH (B), both with 1% (v/v) formic acid. Elution program: Isocratic at 48% B for 2.2 min, linear gradient to 80% B from 2.2-74.8 min, linear gradient to 100% B from 74.8-77.0 min, isocratic at 100% B from 77.0-88.0 min.

### **Preparative RP-HPLC-ESI-MS**

For preparative HPLC, samples were injected on a Waters XBridge Prep C18 OBD column (19  $\times$  250 mm, 5  $\mu\text{m}$  particle size) (Waters, Milford, MA, USA) and eluents used were water (A) and ACN (HPLC-R grade) (B), both with 1% (v/v) formic acid. The elution programs for the different compounds were as follows:

**Compound 1:** Isocratic at 37% B for 3.68 min, linear gradient to 47% B from 3.68-38.68 min, linear gradient to 100% B from 38.68-42.18 min, isocratic at 100%B from 42.18-59.69 min, linear gradient to 37% B from 59.69-63.19 min, isocratic at 37% B from 63.19-80.96 min.

**Compounds 2, 3, 4 and 5:** Isocratic at 38% B for 3.68 min, linear gradient to 48% B from 3.68-38.68 min, linear gradient to 100% B from 38.68-42.18 min, isocratic at 100% B from 42.18-59.69 min, linear gradient to 38% B from 59.69-63.19 min, isocratic at 38% B from 63.19-80.96 min.

**Compound 6:** Isocratic at 42% B for 3.68 min, linear gradient to 52% B from 3.68-38.68 min, linear gradient to 100% B from 38.68-42.18 min, isocratic at 100% B from 42.18-59.69 min, linear gradient to 52% B from 59.69-63.19 min, isocratic at 52% B from 63.19-80.96 min.

**Supplementary data** with “Antibacterial activity of prenylated stilbenoids from peanut” by de Bruijn, Araya-Cloutier, Bijlsma, de Swart, Sanders, de Waard, Gruppen, and Vincken

#### **Analytical RP-UHPLC-PDA-ESI-IT-MS<sup>n</sup>**

For analytical UHPLC coupled to ESI-IT-MS<sup>n</sup>, samples were injected on a Waters Acquity BEH C18 2.1 × 150 mm, 1.7 μm particle size column with a Waters VanGuard 2.1 × 5 mm guard column of the same material. Eluents used were water (A) and MeOH (B), both with 0.1% (v/v) formic acid. Elution program: Isocratic at 48% B for 1.45 min, linear gradient to 80% B from 1.45-16.96 min, linear gradient to 100% B from 16.96-18.42 min, isocratic at 100% B from 18.42-25.96 min. The eluent was adjusted to its starting composition in 1.18 min, followed by equilibration for 7.27 min.

#### **Analytical RP-UHPLC-PDA-ESI-FTMS**

For analytical UHPLC coupled to ESI-FTMS, samples were injected on a Waters Acquity BEH C18 2.1 × 150 mm, 1.7 μm particle size column with a Waters VanGuard 2.1 × 5 mm guard column of the same material. eluents used were water (A) and ACN (B), both with 0.1% (v/v) formic acid. Elution program: Isocratic at 20% B for 0.58 min, linear gradient to 100% B from 0.58-47.18 min, isocratic at 100% B from 47.18-50.10 min.

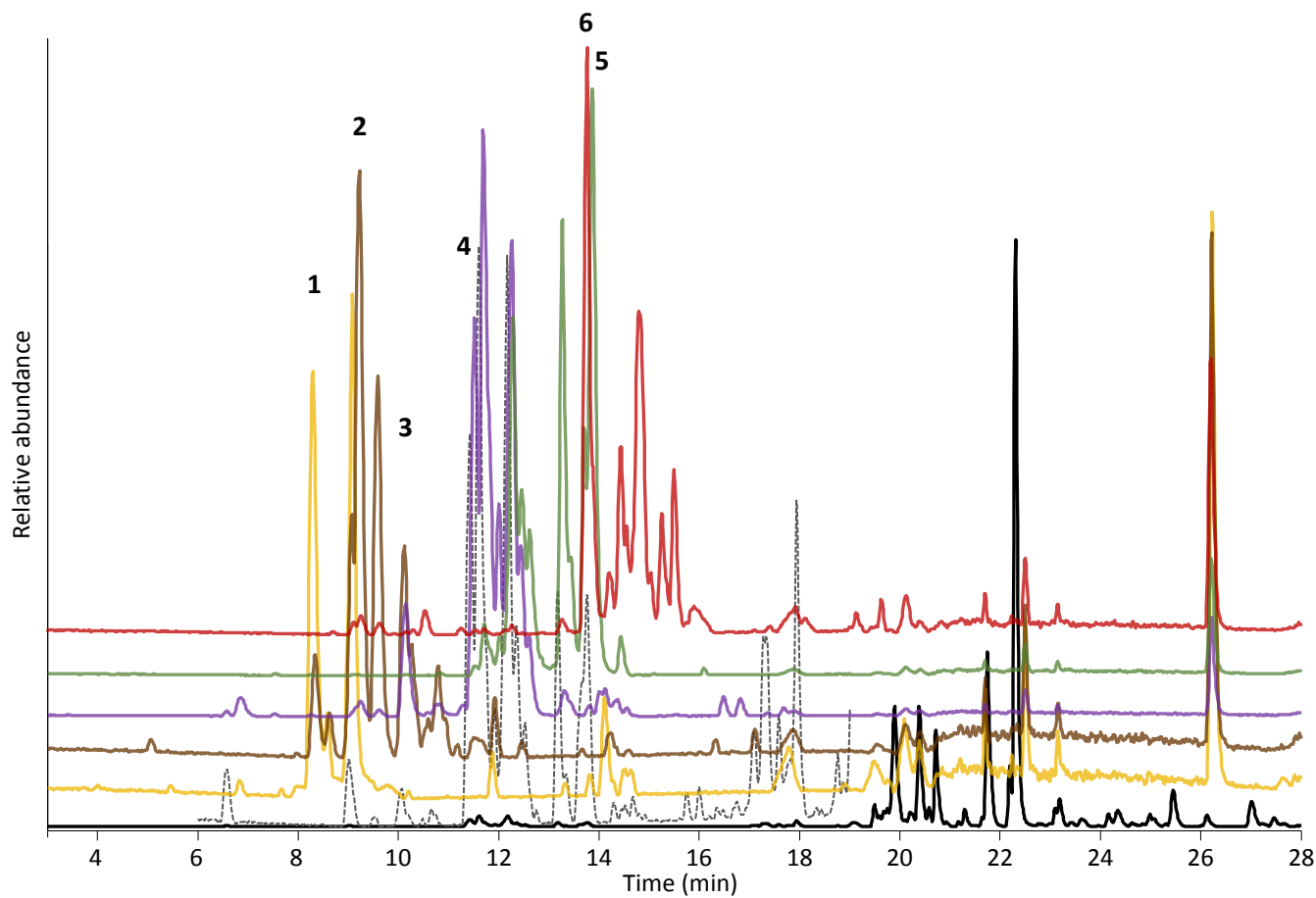


**Figure S1.** UHPLC-ESI-IT-MS negative mode ( $m/z$  250-1000) chromatograms of cleaned peanut extract (black, full chromatogram; grey-dashed, zoom of 6-19 min) and pools obtained after Flash chromatography. Yellow, pool with compound **1**; brown, pool with compounds **2** and **3**; purple, pool with compound **4**; green, pool with compound **5**; and red, pool with compound **6**.

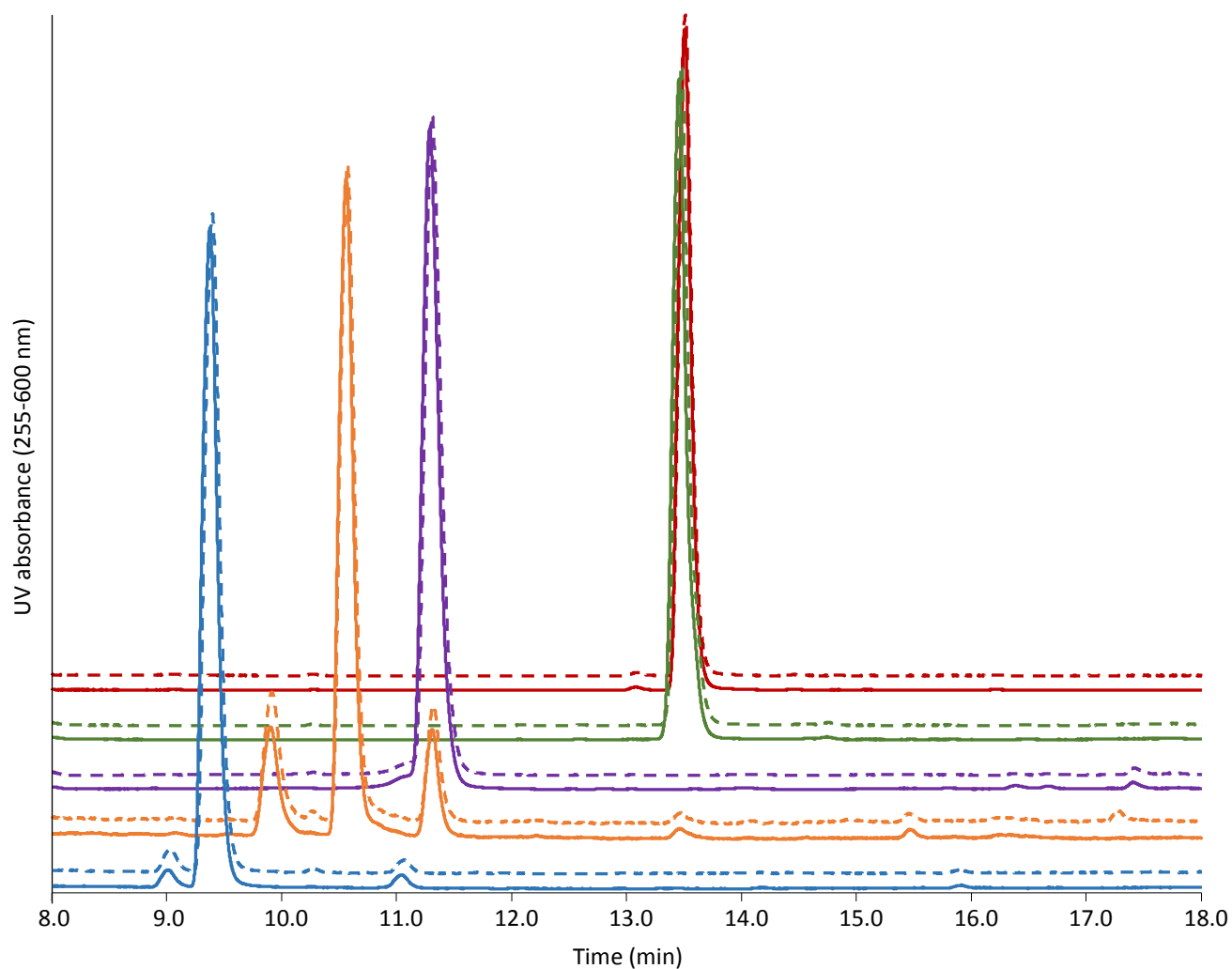


**Figure S2.** UHPLC-PDA (255-600 nm) chromatograms of compounds **2**, **3**, **4**, **5** and **6** before (solid line) and after (dashed line) incubation for 24 h under antimicrobial assay conditions. Blue, arachidin-2 (**2**); orange, arachidin-3 (**3**); purple, arachidin-6 (**4**); green, arahypin-5 (**5**); and red, chiricanine A (**6**).